Characterization of a transient collisional Ni-like molybdenum soft-x-ray laser pumped in grazing incidence

S. Kazamias,* K. Cassou, D. Ros, F. Plé, G. Jamelot, and A. Klisnick
LIXAM, UMR 8624, Université Paris Sud, F-91405 Orsay Cedex, France

O. Lundh, F. Lindau, A. Persson, and C.-G. Wahlström
Department of Physics, Lund University, S-22100 Lund, Sweden

S. de Rossi and D. Joyeux
Laboratoire Charles Fabry de l'Institut d'Optique, Campus Polytechnique, RD 128, F-91127 Palaiseau, France

B. Zielbauer, D. Ursescu, and T. Kühl
Gesellschaft für Schwerionenforschung (GSI), D-64291 Darmstadt, Germany
(Received 27 July 2007; published 6 March 2008)

We present experimental results from an extensive investigation of a Ni-like Mo x-ray laser pumped in the transient regime and GRIP configuration (GRazing Incidence Pumping). The pump laser is a 10 Hz, 1 J, Ti:sapphire laser system. The main diagnostic is a monochromatic near-field imaging system with a 1.7 micron spatial resolution that shows the soft-x-ray laser source size and position relative to the target surface. Changes of those characteristics are observed for different GRIP angles, varied between 15° and 21°, while keeping all other parameters constant. Intense lasing is observed routinely at 18.9 nm with up to 3 microjoule output energy and stable operation is demonstrated at 10 Hz. We have investigated the role of several pumping parameters, in particular, the relative energy and delay between the long and short pulse. We show that this multiparameter scan leads to a well-defined optimal regime of operation and better understanding of the GRIP configuration. Finally, as the GRIP scheme requires careful tailoring of the plasma conditions to the specific soft-x-ray laser under investigation, we add a prepulse before the plasma producing long pulse to generate large-scale preplasmas. This increases the brightness of the soft-x-ray beam and leads to an almost Gaussian near-field spatial profile.

DOI: 10.1103/PhysRevA.77.033812 PACS number(s): 42.55.Vc, 32.30.Rj, 42.60.Da, 52.50.Jm

I. INTRODUCTION

Since the mid-1990s, intense and successful efforts, both experimental and theoretical, have been done in soft-x-ray laser research to establish the viability of tabletop pumped devices that would enable the use of this exceptionally bright source in the soft-x-ray spectral domain for applications at the university scale.

The soft-x-ray laser research field is currently experiencing a rapid development since the first demonstration of high repetition rate transient soft-x-ray laser from solid target by Keenan *et al.* [1] who used a Ti:sapphire laser as the pump laser. They also showed the advantage of the so-called GRazing Incidence Pumping (GRIP) configuration for which the plasma is pumped at grazing incidence and the pump laser is refracted in the plasma. This first demonstration was followed by the work of other groups [2–5] who obtained the saturation of different kinds of soft-x-ray lasers at various wavelengths down to 11 nm.

The GRIP configuration has many advantages over the normal incidence pumping [6]: in particular, the grazing angle is a new parameter that can be adjusted to match the energy deposition and plasma heating to the optimum zone for gain. As the density in the plasma where the energy is absorbed becomes smaller when the grazing angle is reduced, there should also be less density gradient in this region. This should improve the propagation of the soft-x-ray laser beam in the amplifying medium. It is therefore of great importance to precisely investigate the effect of GRIP angle on the plasma and soft-x-ray laser characteristics and to make possible comparisons with detailed quantitative simulations. This will increase the physical understanding of GRIP systems, which is crucial for their optimization and their use as an amplifier medium for coherent radiation such as high order harmonics [7,8] or as a direct source for applications.

During an experimental campaign on the 10 Hz, 35 TW Ti:sapphire laser system at the Lund Laser Center in Sweden, we used the GRIP configuration to produce a saturated soft-x-ray laser at 18.9 nm from a Ni-like molybdenum plasma generated on a 4 mm solid target [9]. By high resolution near-field imaging of the soft-x-ray laser source, we investigated in detail the effect of the GRIP angle on the soft-x-ray laser output characteristics such as integrated energy, vertical and horizontal size, and emission distance from target surface. This was done for a large set of parameters such as the delay between the long and short pulse and their relative energy but also the presence of a small prepulse, before the long pulse that creates the plasma, was investigated.

After a detailed description of the experimental setup in Sec. II, the rest of the paper will be dedicated to the study of

*sophie.kazamias@u-psud.fr

 ©2008 The American Physical Society

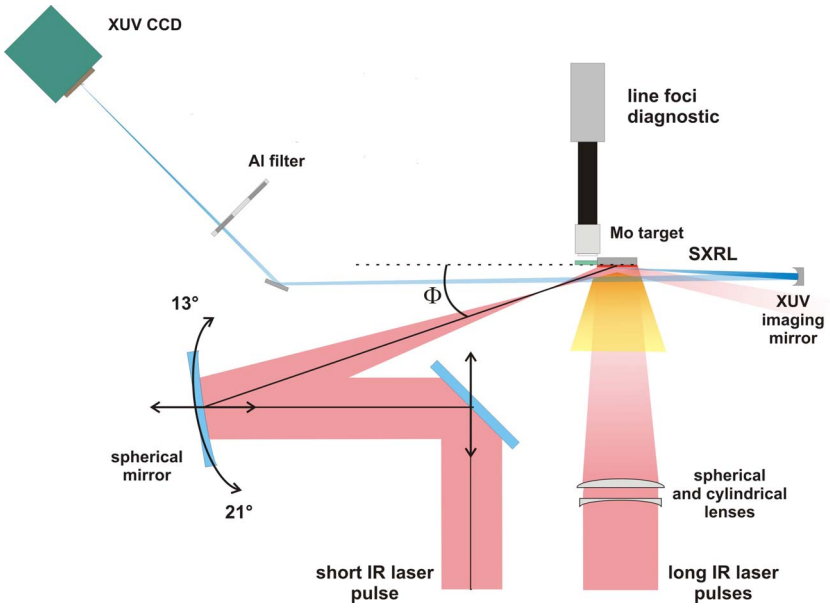

FIG. 1. (Color online) Schematic top view of the experimental setup.

first the influence of grazing angle (Sec. III), then the influence of the delay between the two main laser pulses (Sec. IV) and the effect of a small prepulse before the long pulse (Sec. V). We will conclude on the best characteristics obtained for this source in terms of energy in the soft-x-ray laser pulse, size, position, etc. (Sec. VI).

II. EXPERIMENTAL PRINCIPLE AND CONFIGURATION

The pump laser for the following study of soft-x-ray laser generated in GRIP configuration is the 30 TW laser system of the Lund Laser Center in Sweden. It is a chirped pulse amplification (CPA) Ti:sapphire laser system that usually delivers 1 J in 35 femtosecond (fs) pulses at 10 Hz repetition rate and 800 nm central wavelength. For the soft-x-ray laser generation, the 1.4 J of uncompressed energy is split after the last amplifier stage into two beams with adjustable energy ratio. One of the beams, the so-called long pulse (LP), remains uncompressed, with 300 ps duration and is used to create the plasma. The other one, the so-called short pulse (SP), enters the compressor and is compressed down to 5 ps to heat the plasma and pump the soft-x-ray laser transition. We found that the best condition corresponds to the same energy level for the long and short pulse: approximately 500 mJ on target in each arm.

A low energy prepulse generator was installed in the long pulse beam path to allow additional control of the preplasma conditions. The device is composed of a combination of a half-wave plate and a cube polarizer and is designed to vary continuously the energy balance between the prepulse and the long pulse, from 0 to 100%. However, the smallest prepulse energy level that is practically obtained was 7% due to the polarizer quality. At this low level, the noise on the photodiode is rather large and the energy evaluation is given with large fluctuations. The maximum delay between the pulses is given by the size of the delay line and reaches 2.4 ns. For most of the experiment, the prepulse preceded the long pulse by 1.3 ns and contained 7% of its energy but results obtained in significantly different conditions will also be discussed in this paper. All of these beams were focused in line on a 4-mm-long molybdenum slab target.

The focusing system for the long pulse(s) with a 17 mm beam diameter consisted of a combination of a cylindrical ($f=-4$ m) and a spherical ($f=1$ m) lens. The position of the latter was adjusted to vary the width of the focal line. The length of the line focus was 6 mm and led to irradiance on targets of 2.9×10^{10} W cm^{-2} and 3.8×10^{11} W cm^{-2} for the 7% prepulse and the long pulse, respectively. The focusing system for the short pulse with a 50 mm beam diameter and incident on target at grazing incidence, was composed of a spherical mirror ($f=650$ mm) whose incidence angle was adjustable under vacuum between 7.5° and 10.5° to lead to GRIP angle Φ, on target between 15° and 21°. The focal line length, which only depends on beam diameter and grazing angle, was between 5 and 9 mm, whereas its width was approximately 40 μm. An important point is that the spherical mirror position, together with the 45° mirror before it (see Fig. 1), were adjustable under vacuum to maintain the target position and direction constant while changing the GRIP angle. The superposition and shape of the focused beams were controlled with an imaging microscope with a resolution reaching 3 μm. The delay between the pulses was adjustable under vacuum, from 100 to 800 ps with 100 ps time resolution, using a delay line placed in the long pulse beam path. This setup design is different from the one presented, for example, in Ref. [3] where the GRIP angle was varied by rotating the target. This technical solution leads to better quality focusing and superposition of the focal lines. It is also required when using high resolution diagnostics of the plasma and soft-x-ray laser.

The main diagnostic shown in Fig. 1 is a two-dimensional (2D) soft-x-ray near-field imaging system composed of a f

=500 mm multilayer spherical mirror coated for spectral selection at the soft-x-ray laser wavelength (Institut d'Optique design and manufacturing). To get a very high resolution with low astigmatism, the mirror is used at the minimum available incidence angle (0.7°) to allow the beam redirection by a flat mirror placed at the center of the vacuum chamber. After more than 4 m propagation, the magnified image of the soft-x-ray laser source, at the exit plane of the plasma, is detected on a calibrated 16-bit back thinned soft-x-ray charge coupled device (CCD) camera. The resolution given by the system is 1.7 μm and corresponds to a magnification factor of 7.6. A set of aluminum filters with thicknesses between 1 and 6 μm was placed in the soft-x-ray laser beam to adjust the intensity level. The 6 μm filter was used in most of the experimental configurations, indicating in itself a high signal level for the soft-x-ray laser output.

The high repetition rate operation of this soft-x-ray laser allows one to perform a complete series of multidimensional parameter optimization. The recorded images were carefully analyzed to extract physical quantities such as the integrated energy, the horizontal and vertical widths of the source, and its distance from the target surface. The mean fluence of the source could then be derived from the measured data, as well as the mean peak intensity when assuming a pulse duration of 5 ps, as measured in a similar experiment [10]. All the measurements presented below are the result of an average over at least five shots recorded in the same experimental conditions. A recent paper [11] presents in detail the 10 Hz operation of this type of soft-x-ray laser as a source for applications: it shows that soft-x-ray laser output characteristics depend on the target operation, static or moving, and target preparation through the level of oxidation and surface roughness. The soft-x-ray laser output stability is also directly dependent on the pump laser stability in terms of energy and beam pointing.

III. INFLUENCE OF THE GRIP ANGLE

The behavior of the soft-x-ray laser output as a function of the short laser pulse grazing angle is presented in Fig. 2. The delay between the long and short pulses is fixed to Δt_{LP-SP}=400 ps, which corresponds to the optimum measured delay for most of the angles Φ between 15° and 21° as will be shown in the next section. Note that working at a fixed delay Δt_{LP-SP}, allows one to study the interaction of the short pulse with the same preplasma conditions whatever the GRIP angle. As was briefly presented in a recent letter [9], the mean output fluence shows a clear optimum for a 19° GRIP angle and reaches 0.33 J/cm^2, which corresponds to an integrated soft-x-ray laser energy up to 3 μJ.

The distance of the source from the target surface also varies significantly with the GRIP angle: it first decreases from 60 to 35 μm for angles between 15° and 19°, then increases to around 50 μm for larger ones until 21°. Such a trend was expected since the pump laser beam penetrates deeper in the plasma and is absorbed at higher electron density when the GRIP angle is increased, following the well-known mirage formula $n_e=n_c \sin^2 \Phi$, where n_e is the electron density of the plasma and n_c is the critical density for

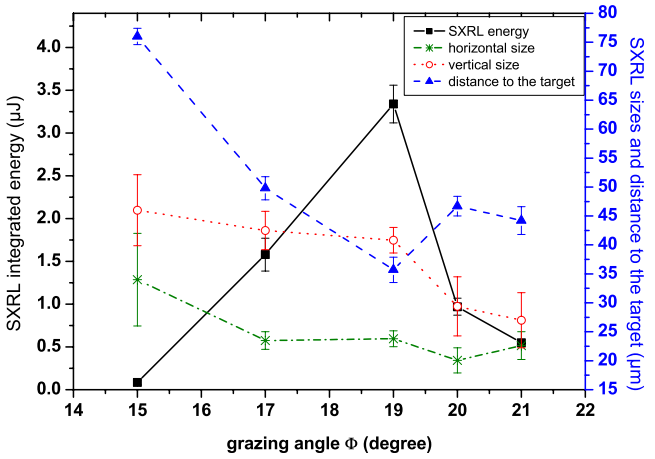

FIG. 2. (Color online) Grazing angle effect on the soft-x-ray laser integrated energy, position relative to the target surface, (FWHM) horizontal and vertical widths.

the laser wavelength [6]. In our case, n_e is just below 1.8 $\times 10^{20}$ cm^{-3} for a 19° GRIP angle. Above the optimum grazing angle, the soft-x-ray laser source aperture is shifted to larger distances. This can be interpreted as due to a stronger refraction of the IR laser beam followed by a spatial reshaping of the gain zone, since absorption occurs at a higher density where the density gradient is steeper. As additional information on the grazing angle effect, both horizontal and vertical sizes of soft-x-ray laser pupil are reduced when increasing the grazing angle. Pumping in a denser plasma region should indeed correspond to a decrease of the plasma scale length ($L=n_e/\nabla n_e$). Numerical simulations performed for similar pumping conditions but for a different lasing element tend to indicate that the 19° GRIP angle corresponds to an electronic density for which the density profile experiences a steeper increase along the horizontal axis [6], leading to a more dramatic increase of the density gradient. The fine study and understanding of the influence of electronic density gradients on the gain zone creation would require more detailed simulations.

The optimum GRIP angle is thus a compromise between absorption at high electron density and low electron density gradient together with a high abundance of Ni-like ions. An important experimental result is that the optimum angle is observed at the same value for a wide range of other experimental parameters such as delay between the short and long pulse, energy balance between them, and focusing geometry.

IV. INFLUENCE OF THE HEATING DELAY

We discuss in this section the influence of the peak-to-peak delay between the long and short pump pulses, on the shape and energy of the soft-x-ray laser source. For increasing delays, plasma expands and the dense area of interest ($5\times 10^{19} \leq n_e \leq 1\times 10^{21}$ cm^{-3}) cools down. As a result, the electron density gradient decreases in time, mainly along the horizontal axis normal to the target surface.

Figure 3 shows the integrated soft-x-ray laser energy as a function of the delay, from 50 to 850 ps for five GRIP angles

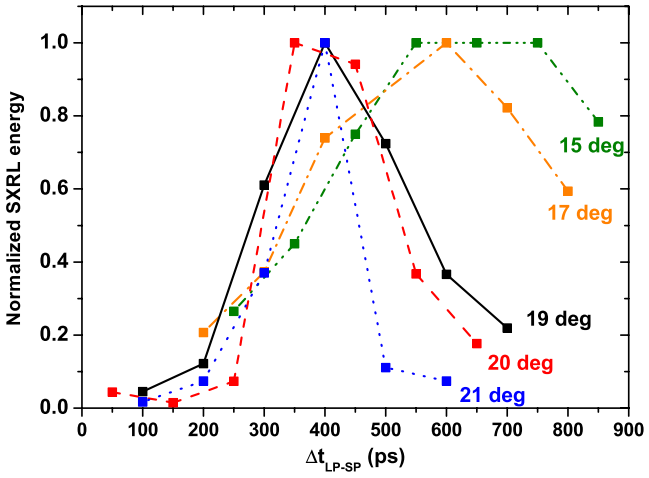

FIG. 3. (Color online) Normalized soft-x-ray laser energy, for a grazing angle from 15° to 21°, as a function of the delay between long pulse and short pulse.

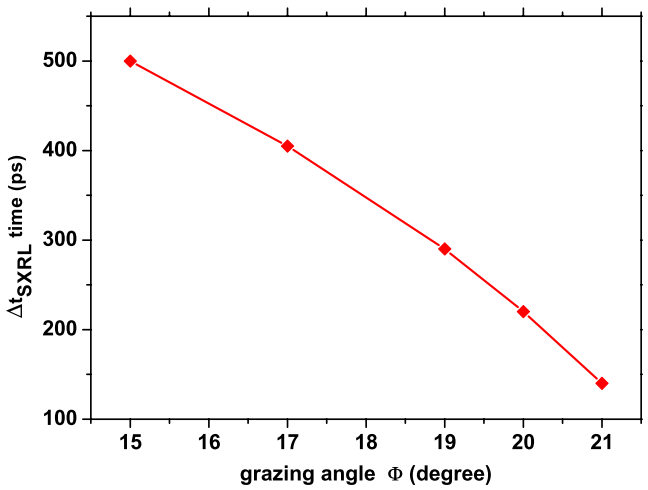

FIG. 4. (Color online) Full width at half maximum duration of the soft-x-ray laser delay window over which efficient lasing is observed.

between 15° and 21°. In order to make the comparison between different GRIP angles easier, the values shown in Fig. 3 are normalized to the maximum for each series corresponding to a given angle. Each point on this figure corresponds to the average over several shots, typically 5–10, with fluctuations of the order of 10–30 % depending on the signal level as explained in detail in Ref. [11]. It can be seen that for the smallest angles the optimum delay is around 600 ps ($\Phi = 15° \rightarrow \Delta t_{LP-SP} = 700$ ps, $\Phi = 17° \rightarrow \Delta t_{LP-SP} = 600$ ps), while it is around 400 ps for the grazing angle 19° and above. Note that, at optimum delay, the short pulse is always largely after the end of the long pulse whose duration is 300 ps: in other words, the soft-x-ray laser is really pumped sequentially by separated pulses playing distinct roles. Another interesting feature exhibited in Fig. 3 is that the delay interval during which lasing is obtained, is much larger for small angles than for larger ones. Actually this delay interval constantly decreases when increasing the GRIP angle, as shown in Fig. 4.

The falloff of the soft-x-ray laser energy at the shortest delays can be explained by steep density gradients in a plasma which has not had enough time to expand and thus allows the efficient propagation of both the pumping laser pulse and the soft-x-ray laser beam. It can be seen in Fig. 3, that this effect is more crucial for larger GRIP angles such as $\Phi = 20$ and 21° that exhibit almost no signal for delays shorter than 250 ps whereas for $\Phi = 15$ and 17° the signal for 200 ps is still not negligible as compared to the maximum value (20%).

On the other hand, the falloff of the soft-x-ray laser energy toward longer delays is controlled by plasma cooling and recombination. In those cases, the short pulse is indeed incident in a plasma where the temperature and the average ionization have decreased, resulting in a lower density of lasing ions and, hence lower gain. This effect is more pronounced at higher electron density (recombination rates are higher), i.e., when the GRIP angle is larger. This explains why the delay interval for lasing is reduced for larger GRIP angles, as represented in Fig. 4.

The fact that refraction is the main mechanism which prevents lasing for the shortest delays is also confirmed by the near-field images shown in Fig. 5. For the shortest delay, 200 ps, the soft-x-ray laser source has a vertical double structure which is likely to be induced by refraction in the vertical direction of the IR pump beam. Such double structures were reproducibly observed for delays below 250 ps, but disappeared for larger delays, as shown in Fig. 5.

In conclusion, varying both delay Δt_{LP-SP} and GRIP angle, gives rise to a complex behavior of preplasma as it interacts with the short laser pumping pulse. The optimum delay for soft-x-ray laser emission is governed by a compromise between refraction for short delays and dense plasma cooling for longer ones. The sensitivity of amplification to the delay increases with the GRIP angle.

V. INFLUENCE OF PREPLASMA CONDITIONING AND PREPULSE EFFECTS

The importance of adding a low-energy prepulse a few nanoseconds before the main long pulse, which creates the plasma, is well known since the first experimental demonstrations of soft-x-ray laser pumped in the quasi-steady-state regime in the mid-1990s [12–14]. Simulations performed for the transient collisional scheme for normal [15] or longitudinal incidence [16] also confirm the relevance of this tech-

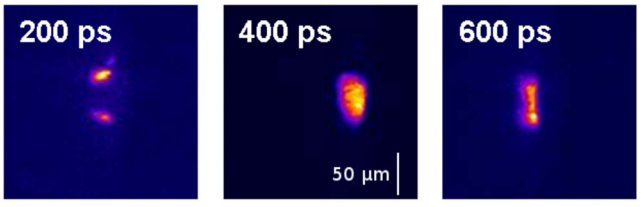

FIG. 5. (Color online) Near-field images for different delay between the long and short laser pulses. Experimental conditions were $\Phi = 19°$, and the IR energy balance was 500 mJ on each arm.

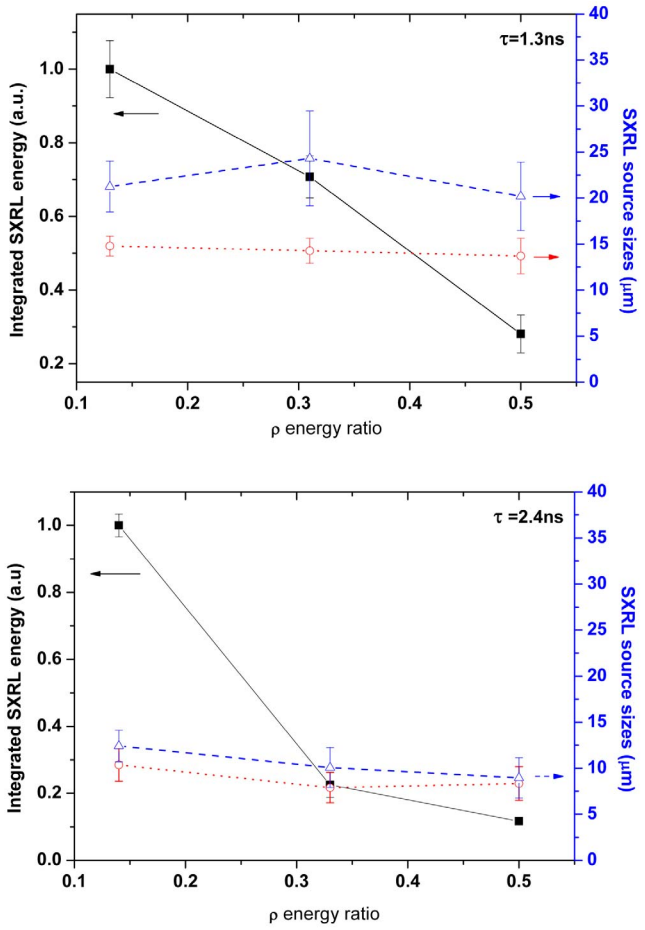

FIG. 6. (Color online) Soft-x-ray laser source characteristics (solid square: normalized integrated energy; open triangle: vertical size; open circle: horizontal size) for optimized conditions $\Delta t_{LP-SP}=400$ ps with prepulse delays $\tau=1.3$ ns (a) and $\tau=2.4$ ns (b) at variable energy ratio ρ, between prepulse and long pulse.

nique to shape an ideal preplasma for soft-x-ray laser generation. By adding a prepulse, the plasma interaction volume increases by hydrodynamic expansion. This leads to a reduction of the density gradient and an increase of the absorption of the main pulse. When working in the GRIP geometry, the use of a low-energy prepulse hence allows one to efficiently heat the plasma at the optimum density where the lasing ions are abundant, together with a reduced density gradient.

The prepulse generator, as described in Sec. II, allows the delay τ between the prepulse and the long pulse, and the energy ratio ρ between them ($\rho=E_{prepulse}/E_{long\ pulse}$) to be varied. The total energy $E_{prepulse}+E_{long\ pulse}$ and the GRIP angle $\Phi=19°$ were kept constant for the following study. Note that $\rho=10\%$ corresponds to an irradiation level on a target of 4×10^{10} W/cm^2.

From the optimized conditions described in previous sections, we first varied the so-called contrast from 7% to 50% at a fixed delay between prepulse and long pulse ($\tau=1.3$ ns) and fixed total pump energy. The results are shown in Fig. 6(a): no significant change as a function of ρ was observed on the soft-x-ray laser source size, neither vertical nor horizontal. We rather noted an increase of the source

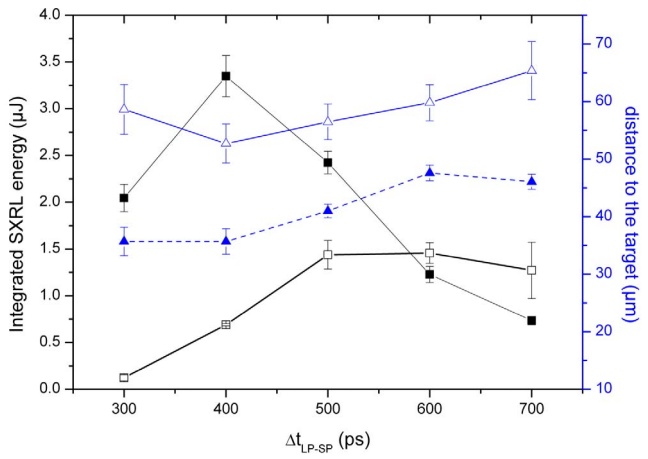

FIG. 7. (Color online) Comparison of the soft-x-ray laser source characteristics for optimized conditions with a prepulse delay $\tau=2.4$ ns [open symbol, case of Fig. 6(b)] and $\rho=14\%$ and $\tau=1.3$ ns [solid symbol, case of Fig. 6(a)] and $\rho=7\%$ at variable delay between long pulse and short pulse. The squares show integrated energy and the triangles show distances to the target surface.

instability and even an energy reduction for large ρ values. The latter might be attributed to the fact that the total energy between prepulse and long pulse is kept constant and thus that increasing ρ means consequently decreasing the long pulse irradiation level on target, reaching a real multipulse irradiation scheme. Figure 6(b) shows the same phenomenon at a larger delay ($\tau=2.4$ ns) and confirms that only changing the prepulse energy ratio, without changing the delay, has no real impact on the geometrical soft-x-ray laser characteristics.

The importance of preplasma conditioning through the increase in delay between prepulse and long pulse can be understood thanks to the two following experimental facts: first, as shown in Fig. 7, the source position is strongly influenced by τ: changing τ from 1.3 to 2.4 ns, the distance to the target increases from 35 to 55 μm. Second, when varying the second delay Δt_{LP-SP} between the long and short pumping pulse for $\tau=1.3$ and 2.4 ns, the soft-x-ray laser energy reduction at large delays attributed in Sec. IV to dense plasma cooling, is more important for small τ. These observations confirm that the preplasma effect is governed by plasma hydrodynamic expansion and that increasing τ leads to the shift of the gain region toward low density regions of the plasma together with low gradients.

Finally, the main interesting feature shown by comparing Figs. 6(a) and 6(b), and already reported in [9], is that the soft-x-ray laser source dimension in both directions is significantly reduced when the prepulse to long pulse delay goes from 1.3 to 2.4 ns. This source size reduction is also accompanied by an energy reduction: a factor of 2 in our case. We observed experimentally that the source size is more critical on the fluence than purely the source energy (quadratical variation for the geometrical aspect). Although this behavior is not yet fully understood, it yields a very interesting level of source fluence up to 1.2 J/cm^2 as compared to approximately 0.3 J/cm^2 in the usual energy-

optimized case. For some applications such as irradiation experiments, where the relevant parameter is more the source fluence than the integrated energy [17], such a result is hence of high interest.

As a preliminary conclusion, the addition of a small prepulse before the long pulse with the appropriate delay may increase significantly the source fluence and quality. We observed that the delay has more effect on the source geometry than simply changing the prepulse energy level. Detailed multiscan experimental optimization of this prepulse effect should be further explored.

VI. CONCLUSIONS

In conclusion, we have performed experiment and here reported on an extensive multiparameter optimization of a transient Ni-like Mo soft-x-ray laser at 18.9 nm, pumped under grazing incidence. By imaging the soft-x-ray laser at the output of the plasma rod, we obtain, for the first time, detailed insight on the effect of varying the GRIP angle among other parameters. We demonstrate that varying the GRIP angle strongly influences the pump laser coupling into the plasma: the soft-x-ray laser output energy is indeed reduced by more than one order of magnitude when changing the GRIP angle by only a few degrees around the best position, found to be close to 19°.

Moreover, we show that the soft-x-ray laser source shifts closer to the target when increasing the grazing angle, which directly demonstrates the concept of GRIP: the density at which the soft-x-ray laser is generated can be varied with the GRIP angle. For angles larger than optimum value, refraction of both the pump and soft-x-ray laser beams seems to play an important role. The optimization versus the delay between the long and short pulses led to a clear optimum at 400 ps in almost any experimental configuration, including, in particular, different GRIP angle values. An interesting result is that the range of delays over which an important soft-x-ray laser emission is observed decreases with the GRIP angle: increasing this parameter thus makes the delay optimization more critical.

Finally, our preliminary results on the effect of a weak prepulse to shape the preplasma indicate that the delay between prepulse and long laser pulse is a more critical parameter to control than only the energy level. For long prepulse delay (τ) condition and increased prepulse energy of $\approx 10\%$ corresponding to an intensity of $\approx 4 \times 10^{10}$ W/cm^2. As also mentioned in Ref. [9] we observe soft-x-ray laser sources with an exceptionally high brightness level.

This detailed study of the physics of the soft-x-ray laser, pumped in grazing incidence, should give useful benchmarks for numerical studies to further optimize and understand this type of source that is nowadays the best candidate for simple seeding experiments of high order harmonics in soft-x-ray laser lasers from solid targets [8]. Our work provides a quantitative and accurate characterization of physical quantities which play a crucial role in the optimization of seeding with high order harmonics: the position and size of the active region in the plasma amplifier, as well as the output mean fluence.

ACKNOWLEDGMENTS

This work was supported by the Swedish Research Council, the Knut and Alice Wallenberg Foundation, and through the EU Access to Research Infrastructures activity (Contract No. RII3-CT-2003-506350, Laserlab Europe). Mechanical drawing has been achieved by Jean-Claude Lagron.

[1] R. Keenan, J. Dunn, P. K. Patel, D. F. Price, R. F. Smith, and V. N. Shlyaptsev, Phys. Rev. Lett. **94**, 103901 (2005).
[2] B. M. Luther, Y. Wang, M. A. Larotonda, D. Alessi, M. Berrill, M. C. Marconi, and J. J. Rocca, Opt. Lett. **30**, 165 (2005).
[3] Y. Wang, M. A. Larotonda, B. M. Luther, D. Alessi, M. Berrill, V. N. Shlyaptsev, and J. J. Rocca, Phys. Rev. A **72**, 053807 (2005).
[4] A. Weith, M. A. Larotonda, Y. Wang, B. M. Luther, D. Alessi, M. C. Marconi, and J. J. Rocca, Opt. Lett. **31**, 1994 (2006).
[5] J. Tümmler, K. A. Janulewicz, G. Priebe, and P. V. Nickles, Phys. Rev. E **72**, 037401 (2005).
[6] G. J. Pert, Phys. Rev. A **73**, 033809 (2006).
[7] Ph. Zeitoun, G. Faivre, S. Sebban, T. Mocek, A. Hallou, M. Fajardo, D. Aubert, Ph. Balcou, F. Burgy, D. Douillet, S. Kazamias, G. de Lacheze-Murel, Th. Lefrou, S. Le Pape, P. Mercere, H. Merdji, A. S. Morlens, J. P. Rousseau, and C. Valentin, Nature (London) **431**, 426 (2004).
[8] Y. Wang, E. Granados, M. A. Larotonda, M. Berrill, B. M. Luther, D. Patel, C. S. Menoni, and J. J. Rocca, Phys. Rev. Lett. **97**, 123901 (2006).
[9] K. Cassou, S. Kazamias, D. Ros, F. Plé, G. Jamelot, A. Klisnick, O. Lund, F. Lindau, A. Persson, C.-G. Wahlstrom, S. de Rossi, D. Joyeux, B. Zielbauer, D. Ursescu, and T. Kühl, Opt. Lett. **32**, 139 (2007).
[10] M. A. Larotonda, Y. Wang, M. Berril, B. M. Luther, J. J. Rocca, M. M. Shakya, S. Gilbertson, and Z. Chang, Opt. Lett. **31**, 3043 (2006).
[11] F. Lindau, O. Lundh, A. Persson, K. Cassou, S. Kazamias, D. Ros, F. Plé, G. Jamelot, A. Klisnick, S. de Rossi, D. Joyeux, B. Zielbauer, D. Ursescu, T. Kühl, and C.-G. Wahlstrom, Opt. Express **15**, 9486 (2007).
[12] O. Guilbaud, A. Klisnick, K. Cassou, S. Kazamias, D. Ros, G. Jamelot, D. Joyeux, and D. Phalippou, Europhys. Lett. **74**, 823 (2006).
[13] R. Keenan, C. L. S. Lewis, J. S. Wark, and E. Wolfrum, J. Phys. B **35**, L447 (2002).
[14] B. Rus, Ph. Zeitoun, Th. Mocek, S. Sebban, M. Kalal, A. Demir, G. Jamelot, A. Klisnick, B. Kralikova, J. Skala, and G. J. Tallents, Phys. Rev. A **56**, 4229 (1997).
[15] X. Lu, Y. J. Li, Y. Cang, K. Li, and J. Zhang, Phys. Rev. A **67**, 013810 (2003).
[16] T. Osaki, H. Nakano, and H. Kuroda, J. Opt. Soc. Am. B **19**, 1335 (2002).
[17] S. Kazamias, K. Cassou, O. Guilbaud, A. Klisnick, D. Ros, F. Plé, G. Jamelot, B. Rus, M. Koslova, M. Stupka, Th. Mocek, D. Douillet, Ph. Zeitoun, D. Joyeux, and D. Phalippou, Opt. Commun. **263**, 98 (2006).